ORIGINAL RESEARCH

Protective Effects of Red Ginseng Against Tacrine-Induced Hepatotoxicity: An Integrated Approach with Network Pharmacology and Experimental Validation

Bong-Jo Kim[1], Seon-Been Bak[1], Su-Jin Bae[1,2], Hyo-Jung Jin [ID][3], Sang Mi Park [ID][3], Ye-Rim Kim [ID][3], Dae-Hwa Jung[3], Chang-Hyun Song[3], Young-Woo Kim[1], Sang-Chan Kim[3], Won-Yung Lee [ID][2,4], Sun-Dong Park[1]

[1]Department of Korean Medicine, Dongguk University, Gyeongju, 38066, Korea; [2]Department of Korean Medicine, Wonkwang University, Iksan, 54538, Korea; [3]Medical Research Center, College of Korean Medicine, Daegu Haany University, Gyeongsan, 38610, Korea; [4]Research Center of Traditional Korean Medicine, Wonkwang University, Iksan, 54538, Korea

Correspondence: Won-Yung Lee, Department of Korean Medicine, Wonkwang University, Iksan, 54538, Korea, Email wonyung21@wku.ac.kr; Sun-Dong Park, Department of Korean Medicine, Dongguk University, Gyeongju, 38066, Korea, Email sundong@dongguk.ac.kr

Introduction: Tacrine, an FDA-approved acetylcholinesterase inhibitor, has shown efficacy in treating Alzheimer's disease, but its clinical use is limited by hepatotoxicity. This study investigates the protective effects of red ginseng against tacrine-induced hepatotoxicity, focusing on oxidative stress.

Methods: A network depicting the interaction between compounds and targets was constructed for RG. Effect of RG was determined by MTT and FACS analysis with cells stained by rhodamine 123. Proteins were extracted and subjected to immunoblotting for apoptosis-related proteins.

Results: The outcomes of the network analysis revealed a significant association, with 20 out of 82 identified primary RG targets aligning with those involved in oxidative liver damage including notable interactions within the AMPK pathway. in vitro experiments showed that RG, particularly at 1000μg/mL, mitigated tacrine-induced apoptosis and mitochondrial damage, while activating the LKB1-mediated AMPK pathway and Hippo-Yap signaling. In mice, RG also protected the liver injury induced by tacrine, as similar protective effects to silymarin, a well-known drug for liver toxicity protection.

Discussion: Our study reveals the potential of RG in mitigating tacrine-induced hepatotoxicity, suggesting the administration of natural products like RG to reduce toxicity in Alzheimer's disease treatment.

Keywords: AMPK, liver toxicity, oxidative stress, red ginseng, tacrine

Introduction

Alzheimer's disease, a prevalent and debilitating neurodegenerative disorder, affects approximately 50 million people worldwide, with the number projected to increase to nearly 152 million by 2050.[1] This global health challenge profoundly impacts cognitive function, daily living, and quality of life for affected individuals and their caregivers.[2] Tacrine, an oral acetylcholinesterase inhibitor, has garnered significant attention for its role in the treatment of Alzheimer's disease.[3] By inhibiting the enzyme acetylcholinesterase, tacrine increases the levels of acetylcholine in the brain, thereby ameliorating the cholinergic deficits associated with the disease.[4] However, despite its demonstrated efficacy in alleviating Alzheimer's symptoms, the clinical use of tacrine has been hindered by its toxicity, particularly hepatotoxicity, which affects 30–50% of patients receiving treatment.[5] The hepatotoxicity of tacrine is believed to be associated with the formation of reactive metabolites, leading to oxidative stress and mitochondrial dysfunction in hepatic cells.[6] Consequently, there is a pressing need to identify therapeutic agents that can effectively mitigate the hepatotoxic effects of tacrine, thereby expanding its potential application in the management of Alzheimer's disease and improving patient outcomes.

Red ginseng (RG), a dried and steamed form of *Panax ginseng*, belonging to the family Araliaceae, is renowned for its health-promoting properties and extensive pharmacological potential.[7] Known for its improved digestibility and storage properties compared to raw ginseng, RG has been the focus of various studies investigating its protective effects against oxidative liver injury.[8] Research has shown that RG and its components, such as fermented RG and 20(S)-protopanaxadiol, can exert antioxidative and anti-inflammatory effects on liver tissue, contributing to the overall protection of liver function.[9–11] The unique phytochemical profile of RG, comprising saponins (notably ginsenosides), flavonoids, polyacetylenes, and polysaccharides, underpins its therapeutic potential.[12] Another study suggested that the hepatoprotective properties of RG are exerted through the activation of the AMPK pathway, which defends against oxidative damage and supports liver health.[13,14] Despite these promising findings, the potential of RG to protect against tacrine-induced hepatotoxicity has not yet been fully validated. As such, further investigation is warranted to determine the extent to which RG may serve as a therapeutic agent capable of mitigating the hepatotoxic effects of tacrine, thereby improving the safety and efficacy of this Alzheimer's disease treatment. In this regard, exploring the hepatoprotective potential of natural products, known for their multifaceted bioactive profiles and minimal side effects, becomes paramount.[15,16]

Natural products like RG contain a complex mixture of bioactive compounds that interact with multiple targets, necessitating approaches to reveal their key mechanisms of action. Network pharmacology has emerged as an effective and comprehensive method for investigating complex drug interactions by exploring drug mechanisms within interconnected biological networks.[17] Researchers have combined network pharmacology and experimental validation to study natural products, focusing on synergistic effects, active compound identification, and therapeutic target discovery in complex diseases.[18,19] For example, one study proposed an integrated approach combining multiscale network-level analysis and experimental methods to unraveling the antioxidant properties and active compounds of *Bupleuri Radix*.[20] Another study employed a network-based strategy to explore and validate a flavonoid candidate for non-alcoholic fatty liver disease (NAFLD).[21] Taken together, this integrated approach holds potential for efficiently elucidating the protective effects of RG on tacrine-induced hepatotoxicity and deepening our understanding of the underlying mechanisms involved.

In this study, we aimed to investigate the protective effects of RG against tacrine-induced hepatotoxicity, with a focus on oxidative stress. To achieve this, we integrated network pharmacology analysis with in vitro and in vivo validation. First, A network mapping compounds to targets was constructed for RG, and we delved into its possible advantageous impacts, specifically in the context of oxidative liver injury. Next, in order to evaluate the cytoprotective efficacy of RG against tacrine, we investigated the hepatotoxicity of tacrine and suggested the association with AMPK as a mechanism through the effect of RG on tacrine-induced hepatotoxicity. Subsequently, the protective properties of RG were thoroughly tested using a range of both in vitro and in vivo experiments. This research provides a comprehensive strategy for elucidating the effects of RG on tacrine-induced hepatotoxicity and its system-level mechanisms, highlighting the potential of combining network pharmacological analysis and its validation in the study of natural products and their therapeutic applications.

Materials and Methods
Compound-Target Network Construction
The analysis focused on components that met two criteria: a) alignment with PubChem IDs, and b) having protein target data supported by experimental verification. Verified targets were sourced from several databases, including Drugbank,[22] the Therapeutic Target Database (TTD, version 2.0),[23] and the Search Tool for Interactions of Chemicals (STITCH, version 5.0),[24] along with a compilation by Huang et al.[25] DrugBank and TTD provide extensive information on established and potential targets, associated diseases, pathways, and related drugs. STITCH amalgamates target information for over 430,000 chemicals from multiple resources. Huang et al's work includes a comprehensive collection of both direct and indirect interactions between natural product compounds and proteins, gathered from various databases.

Disease-Associated Proteins
Proteins associated with liver injury and oxidative stress were identified via a STRING PubMed search, utilizing the Cytoscape StringApp plugin.[26] This plugin, based on text-mining technology, helps in identifying proteins linked to specific user queries, making it effective in pinpointing proteins associated with diseases by focusing on particular mechanisms. For instance, in

research targeting protein targets for Parkinson's disease, the emphasis was on neuroinflammation. The query terms used included "liver injury" AND "oxidative stress". Genes/proteins that had co-occurrence scores above a set threshold were identified as proteins linked to liver injury and oxidative stress. This threshold was set higher than in previous studies, at 1, to ensure the selection of reliable related proteins. These chosen proteins were then loaded into Cytoscape 3.7 as a STRING network for additional network analysis.

A hypergeometric test was conducted to assess whether the overlap in proteins between drug targets (like those of ginseng) and disease targets (such as proteins related to oxidative liver injury) was statistically significant or just by chance. The calculation of P-values was based on the following formula:

$$P(k, M, n, M) = 1 - \sum_{i=0}^{k-1} \frac{\binom{n}{i}\binom{M-n}{N-i}}{\binom{M}{N}}$$

In this formula, k represents the count of oxidative liver injury-related proteins among drug targets, M is the total count of drug targets (the number of targets in the compiled dataset), N is the number of drug targets, and n is the count of proteins associated with oxidative liver injury.

Enrichment Analysis on Related Signaling Pathways

Signaling pathways linked to oxidative liver injury identified in literature include AMPK, JAK-STAT, MAPK, NF-kappa B, PI3K-Akt, TNF, toll-like receptor, apoptosis, and protein processing in the endoplasmic reticulum.[27–29] The pathways associated with targets were identified using Enrichr's enrichment analysis tool. Enrichr examined several gene-set libraries, including gene ontology, Kyoto Encyclopedia of Genes and Genomes (KEGG), and Online Mendelian Inheritance in Man (OMIM), to compute adjusted p-values and combined scores for the pertinent gene list (target genes).[30] The combined score was derived from the logarithm of the product of the p-value and z-score. The Benjamini-Hochberg procedure was utilized to address the false discovery rate resulting from multiple tests.

Chemicals and Reagents

Tacrine (9-Amino-1,2,3,4-tetrahydroacridine hydrochloride hydrate) was obtained from Seoul Warehouse South Korea, Korean RG was obtained from Korean Ginseng Corporation (Daejeon, Korea). Dimethyl sulfoxide (DMSO) was purchased from Junsei Chemical (Tokyo, Japan), and Dulbecco's modified Eagle's medium (DMEM), penicillin-streptomycin, and fetal bovine serum (FBS) were supplied from Welgene Inc. (Gyeongsan, Korea). Normocin was purchased from Invivo Gen (San Diego, CA, USA).

Tacrine (9-Amino-1,2,3,4-tetrahydroacridine hydrochloride hydrate) was obtained from Seoul Warehouse South Korea. Dimethyl sulfoxide (DMSO) was purchased from Junsei Chemical (Tokyo, Japan), and Dulbecco's modified Eagle's medium (DMEM), penicillin-streptomycin, and fetal bovine serum (FBS) were supplied from Welgene Inc. (Gyeongsan, Korea). Normocin was purchased from Invivo Gen (San Diego, CA, USA). RG used here was a commercially available extract-type product and kindly provided by Korea Tobacco & Ginseng Corporation (Daejeon, Korea), which is the GMP company approved by Korea FDA and standardized RG according to the Korean Pharmacopoeia.[31] RG was dissolved in the water to treat cells and animals as previously described.[32]

PARP, pro-Caspase3, BCL-XL, β-actin, phospho-AMPK, phospho-ACC, phospho-liver kinase B1 (LKB1), phospho-YAP, Yap and phospho-large tumor suppressor (LATS1) Antibodies against this were purchased from Cruz Biotechnology (Santa Cruz, CA, USA). Cell Signaling Technology (Danvers, MA, USA). Rho123 (Rh123), calcein, propidium iodide (PI), 2',7'-dichlorofluorescein diacetate (DCFH-DA), 3-(4,5-dimethylthiazol-2-yl)-2,5-Diphenyl-tetrazolium bromide (MTT), AICAR and other reagents were purchased from Sigma-Aldrich (St. Louis, MO, USA). The ECL chemiluminescence detection kit was purchased from Amersham Biosciences (Buckinghamshire, UK).

Cell Culture

HepG2 cells, a cell line derived from human hepatocytes, were purchased from ATCC (Rockville, MD, USA), and Hela cells were also from ATCC (Rockville, MD, USA). 10% fetal bovine serum in Dulbecco's modified Eagle's medium (DMEM) FBS, 50 units/mL penicillin, and 50 μg/mL streptomycin at 37°C in a humidified atmosphere containing 5% CO_2. Cells were cultured to reach 80% confluency in a 100mm culture dish, and subcultured at a ratio of 1:3 or 1:4 twice a week with no more than 20 passages.

Cell Viability Analysis (MTT Assay)

HepG2 cells were dispensed at $1×10^9$ cells/well in a 48-well plate, and treated with Tacrine (30, 100, 300, or 1000 μg/mL) alone, followed by MTT after 6 h. Formazan crystals produced by adding 10 μL of MTT (0.1 mg/mL) and incubating for 1 hour were dissolved in DMSO, and absorbance was measured at 570 nm using fluorescence. Likewise, HepG2 cells were dispensed at $1×10^9$ cells/well in a 48 well plate, and then simultaneously treated with Tacrine 300 μg/mL and RG at different concentrations (30, 100, 300, 1000 μg/mL) at 37°C, After 6 hours of culture in a 5% CO_2 incubator, the medium was removed, 10 μL of MTT (0.1 mg/mL) was added, and formazan crystals produced by incubation for 1 hour were dissolved in DMSO and absorbance was measured at 570 nm using fluorescence. Cell viability was expressed as a percentage of control cells. [viability(%control)= $100×$(absorbance of treated sample)/(absorbance of control)].

Fluorescence Microscopy

HepG2 cells were cultured at $1x10^6$ cells/well in a 6 well plate. Tacrine 300 μg/mL and RG 1000 μg/mL were treated together and cultured for 6 hours. Then, Calcein and PI were treated for 1 hour at a concentration of 0.5 μM.

Measurement of Mitochondrial Membrane Permeability (MMP)

MMP was measured using Rh123, a transmembrane fluorescent dye. HepG2 cells were recovered by trypsinization after staining with 0.05 mg/mL of Rh123 for 1 hour. The recovered cells were measured for changes in MMP by Fluorescence-activated cell sorting (FACS) to confirm the viability (BD Accuri™ C6 Plus Flow Cytometer, Seoulin Bioscience).

Immunoblot Analysis

HepG2 cells and Hep3B cells were cultured in a 6 well plate at $1×10^5$ cells/well for 24 h, depleted for 12 h, treated hourly with RG 1000 μg/mL, and then treated with RIPA lysis buffer. A cell lysate was prepared, and the protein concentration was determined using the Micro BCA protein assay reagent kit (Pierce, Rockford, IL, USA) using bovine serum albumin (BSA) as a standard material. The quantified proteins were separated by sodium dodecyl sulfate-polyacrylamide gel electrophoresis (SDS-PAGE) and transferred to a nitrocellulose membrane for subsequent antibody conjugate probing. The nitrocellulose membrane was reacted with primary antibodies such as p-ACC, p-AMPK, p-YAP, YAP, p-LKB1, LKB1 and β-actin, and then treated with secondary antibodies. Immunoreactive protein bands were identified using a Chemi-doc image analyzer (Vilber Lourmat, France) using the ECL chemiluminescence detection kit (Amersham Biosciences, Buckinghamshire, UK).

Animals and Treatment

Animal studies were conducted in accordance with the institutional guidelines of Daegu Haany University, and reviewed by institutional review board (Number: DHU-2022-062) as previously described.[33] Sprague-Dawley rats (140–160 g) were provided by Hyochang Science (Daegu, Korea) and maintained in Daegu Haany University. Rats were divided into five groups. 100 and 300 mg/kg of RG and 200 mg/kg of si lymarin (a positive control) were dissolved in 40% PEG and orally administrated to rats for 3 days. The rats were also orally injected with 30 mg/kg of tacrine in 40% PEG at 1 h after last RG treatment.

Statistical Analysis

Data obtained from independent experiments were analyzed using one-way analysis of variance (ANOVA) or a two-tailed Student's *t*-test. The criteria for statistical significance were set to ***p<0.001, **p < 0.01 and *p < 0.05.
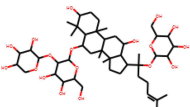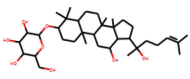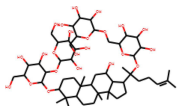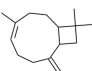
Results

Identification of RG Ingredients and Protein Targets

We first identified RG ingredients and their protein targets from TM-MC and the assembled dataset, respectively. Initially, we discovered 724 compound-target interactions (CTIs) between 42 RG ingredients and 575 protein targets. Among protein targets, NOS2, CASP8, TNF, PTGS2, RELA, IL1B, AR, MAPK1, MMP2, and ROS1 exhibited the highest degrees (9, 8, 8, 7, 7, 6, 5, 5, 5, and 5, respectively). On the other hand, we found that 492 targets interacted with only one RG ingredient. To focus on protein targets associated with enough RG ingredients, we considered 83 targets interacting with two or more ingredients as key targets and conducted subsequent analyses focusing on them.

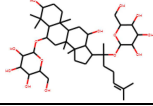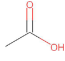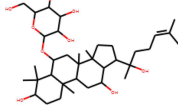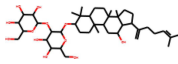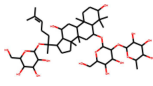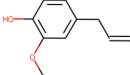### Identification of RG Ingredients and Protein Targets

We first analyzed the intersection of principal targets with proteins associated with oxidative liver injury to examine the correlation between RG targets and proteins linked to disease. It was observed that around 25% of the main targets (20 out of 82) coincided with those associated with oxidative liver injury. To determine if the overlap of these targets exceeded what might occur by chance, a hypergeometric test was utilized. The results revealed that the actual overlap was significantly higher (by a factor of 22.80) than what would be expected randomly (with p-values less than 10^{-20}). This finding suggests a strong connection between RG's primary targets and proteins related to oxidative liver injury, highlighting RG's potential as a protective agent against such liver injury. We next expanded our analysis to determine which ingredients were significantly associated with liver injury (Table 1). The analysis identified 17 ginseng ingredients that were significantly associated with oxidative liver injury. In particular, we found that Notoginsenoside R1, Ginsenoside Rh2, and Ginsenoside Rb1 had the highest overlap ratio with the chance level. This finding suggests that these ingredients may play a crucial role of RG in protecting against oxidative liver injury.

Table 1 Representative Ingredients of RG and Its Association with Oxidative Liver Injury

Name	PubChem CID	Structure	Overlap (Adjusted p-value*)
Notoginsenoside R1	441934		12/19 (1.28E-20)
Ginsenoside Rh2	119307		8/12 (1.25E-14)
Ginsenoside Rb1	9898279		7/10 (2.61E-13)
Caryophyllene	5281515		6/10 (6.88E-11)

(*Continued*)

Table 1 (Continued).

Name	PubChem CID	Structure	Overlap (Adjusted p-value*)
Ginsenoside Rg1	441923		7/18 (2.36E-10)
Acetic acid	176		5/8 (1.6E-09)
Ginsenoside Rh1	12855917		5/9 (4.75E-09)
Ginsenoside Rk1	11499198		3/4 (5.45E-07)
Chikusetsusaponin Ivc	73149		3/5 (2.7E-06)
Eugenol	3314		4/15 (1.56E-05)

Notes: *Indicates p-values adjusted using Bonferroni correction.

Signaling Pathways Associated with RG Targets

Our investigation extended to determining the relevant signaling pathways connected with RG targets. Through an enrichment analysis using the KEGG database, we identified that seven pathways, previously known to be linked to oxidative liver injury, had a significant association with RG's key targets (Table 2). In particular, we noted a close involvement of the AMPK pathway, which is associated with oxidative liver injury through apoptosis induction, with RG's primary targets.28 These results imply that the principal targets of RG play a role in various signaling pathways pertinent to oxidative liver injury, thereby reinforcing its potential as a protective agent against tacrine-induced hepatotoxicity.

Table 2 Significant Enrichment Pathway Related to Oxidative Liver Injury by Key Targets of RG (Adjusted P-value of ≤ 0.05)

Term	Overlap	P-value (Adjusted*)	Combined Score	Related Genes
AMPK signaling pathway	3/120	0.02	27.24	PPAR;SLC2A4;FOXO1
JAK-STAT signaling pathway	5/162	9.45E-4	60.24	IL10;IL6;IFNG;IL2;EGFR
MAPK signaling pathway	16/294	4.08E-13	511.62	TGFB1;BDNF;FOS;MAPK14;TNF;RELA;EGFR;NFKB1; VEGFA;IKBKB;IL1B;CASP3;DDIT3;FAS;MAPK1;TP53
NF-kappa B signaling pathway	8/104	3.78E-08	402.37	NFKBIA;IKBKB;PARP1;IL1B;PTGS2;TNF;RELA;NFKB1
PI3K-Akt signaling pathway	13/354	8.32E-09	211.93	BAD;BDNF;NOS3;IL2;RELA;EGFR;NFKB1;VEGFA;CASP9; IKBKB;IL6;MAPK1;TP53
TNF signaling pathway	16/112	1.95E-19	2263.09	FOS;MAPK14;PTGS2;MMP9;TNF;RELA;NFKB1;NFKBIA; IKBKB;IL6;CASP8;IL1B;CASP3;FAS;CCL2;MAPK1

Notes: *Indicates p-values adjusted using Bonferroni correction.

Compound-Target Network Construction and Visualization

By integrating data on RG's identified components, protein targets, and related pathways, we developed and illustrated RG's compound-target network (Figure 1). This network comprises 232 compound-target interactions (CTIs) involving 83 proteins and 41 RG components. Within this network, the nodes denote the ingredients of RG and their corresponding targets, while the edges refer the interactions between RG's components and protein targets. The count of associated targets for various signaling pathways, including the TNF, MAPK, PI3K-Akt, Toll-like receptor, NF-Kappa B, JAK-STAT, and AMPK pathways, were 16, 16, 13, 11, 8, 5, and 3, respectively. Notably, we observed that certain proteins, like TNF, IL1B, IL6, TP53, NFKB1A, CASP8, CASP9, and CASP3, were concurrently involved in both oxidative liver injury and its associated pathways.

Effect of RG on Hepatocyte Death in Tacrine Hepatotoxicity

The toxicity of tacrine in HepG2 cells was evaluated for cell viability by MTT assay. Treatment with tacrine at concentrations of 30, 100, 300, and 1000 μg/mL resulted in a concentration-dependent decrease in HepG2 cell viability as measured over 6 hours (Figure 2A). At a concentration of 1000 μg/mL, a significant hepatotoxicity of 23.56% was
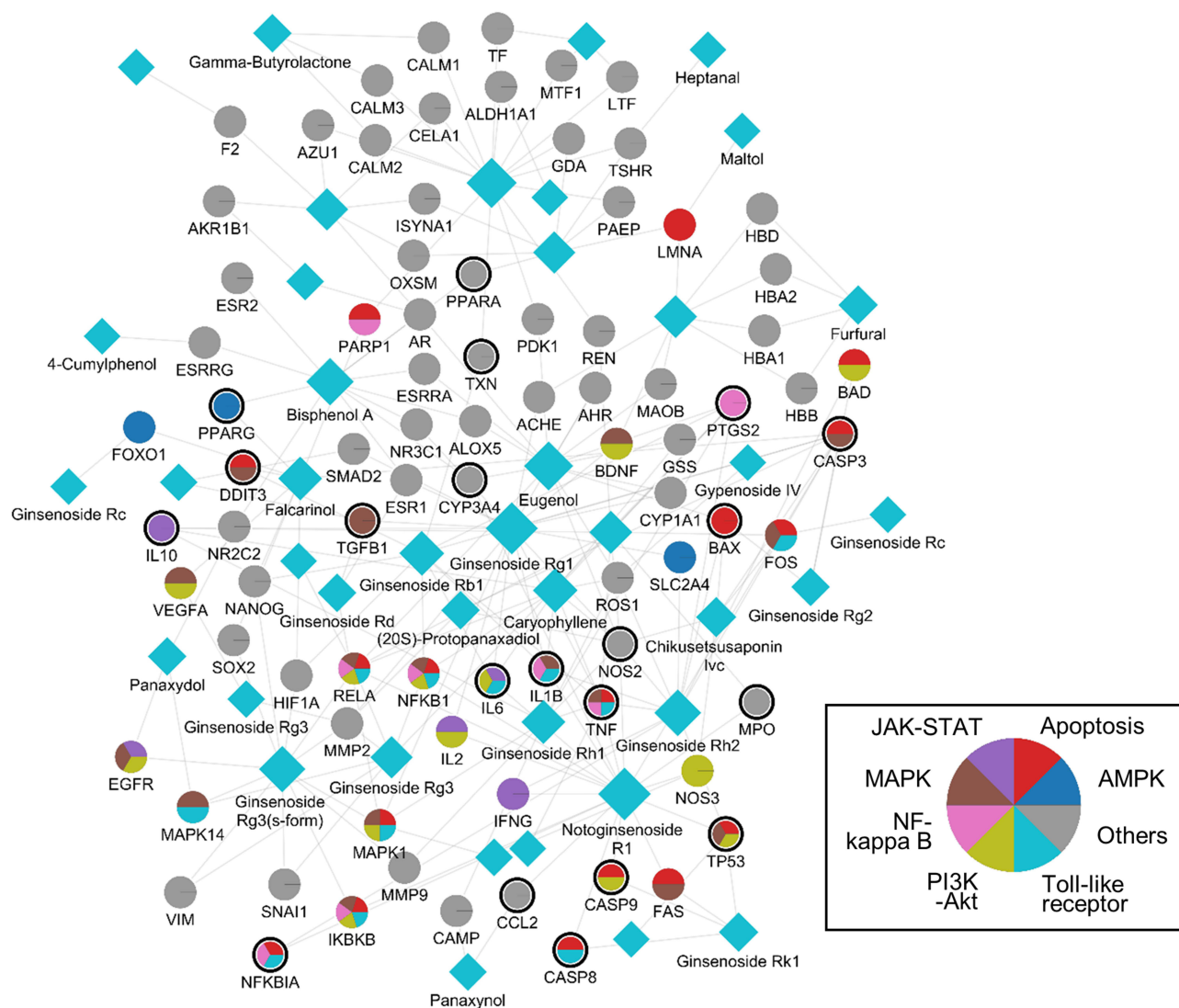

Figure 1 A compound-target network of RG. Circles and diamonds denote protein targets and compounds, respectively. The circle edge and body color indicate targets and signaling path-ways related to oxidative stress and NAFLD, respectively. Edges denote interactions between compound and target.
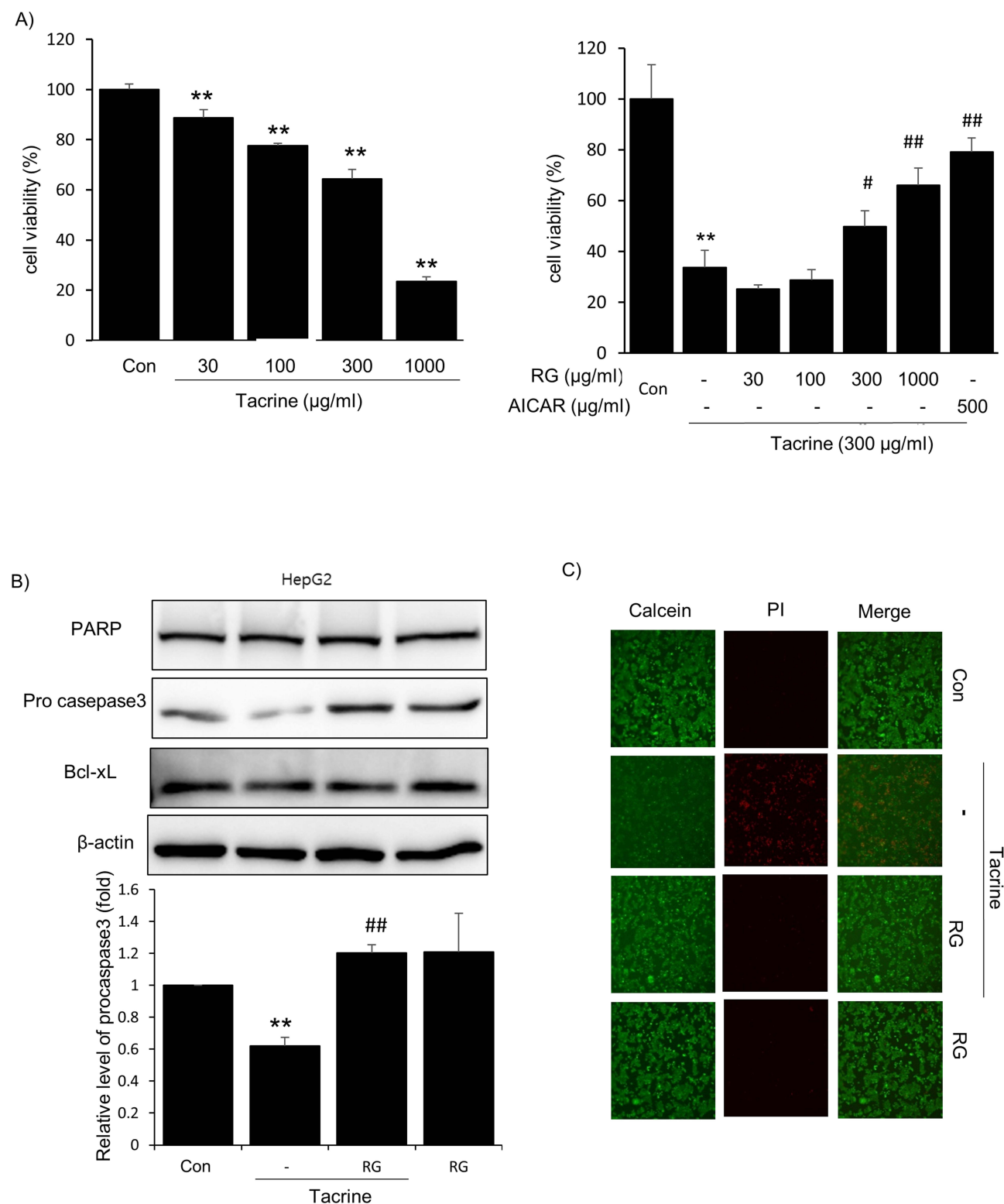
A)

B)

C)

Figure 2 Effect of RG on Tacrine cytotoxicity. (**A**) Effect of tacrine on hepatotoxicity. MTT assay was performed in HepG2 cells. Toxicity of Tacrine (30, 100, 300, 1000 mg/mL) (left), RG (30, 100, 300, 1000 mg/mL) concentration and 300 μM Tacrine were simultaneously administered (right). MTT, 3-(4,5-dimethylthiazol-2-yl)-2,5-diphenyltetrazolium bromide. (**B**) Western blotting of apoptosis-related proteins, PARP, procaspase 3 and Bcl-xL. HepG2 cells were simultaneously treated with 300 μg/mL of Tacrine and 1000 μg/mL of RG for 6 hours. (**C**) The cytoprotective effect of RG was also evaluated under a fluorescence microscope as an experiment to determine the toxicity of Tacrine in hepatocytes. HepG2 cells were treated with RG (1000 μg/mL) and Tacrine (300 μg/mL) for 6 hours. Cells were then stained with Calcein and Pi (0.5 μM each). Data are presented as the average of repeated samples, with error bars representing standard deviations (vs control ** $p < 0.01$; vs Tacrine; [#]$p < 0.05$, [##]$p < 0.01$).

observed. In addition, as a result of examining the internal action of tacrine and RG at the same time, as shown in the graph on the right, the MTT As a result of measuring cell viability by analysis, 1000 μg/mL of RG should be selected as the most significant. In addition, simultaneous treatment with 300 μg/mL of tacrine and 500 μg/mL of AICAI appeared to normalize the cells. Also, to confirm the inhibitory effect of RG on Tacrine hepatotoxicity, MTT assay was followed by immunoblotting of apoptosis-related proteins. Crucial for apoptotic function are executioner caspases, most notably caspase-3, that proteolyze a variety of proteins, inducing cell death.[34] When tacrine was treated in HepG2 cells, there was no change in protein expression in PARP and BCL-XL, but the expression of procase-3 protein decreased, and this reduction was significantly suppressed by RG treatment (Figure 2B). Next, the cytoprotective effect of RG against Tacrine-induced hepatotoxicity was once again confirmed using a fluorescence microscope that observes intracellular fluorescent substances using an ultraviolet light source. After treating cells with 1000 μg/mL of RG and 300 μg/mL of Tacrine for 6 hours, we observed increased PI staining, indicating intense fluorescence and potential cell membrane damage, compared to other groups. These results suggest that RG administration protects the hepatic cells, indicating its potential therapeutic role in mitigating tacrine-induced hepatotoxicity (Figure 2C).

Effect of RG on Mitochondrial Damage in Tacrine Hepatotoxicity

Tacrine-induced hepatotoxicity destroys mitochondrial membrane potential and increases membrane permeability, resulting in apoptosis. Flow cytometric analysis was performed to determine whether RG could prevent apoptosis by disrupting the mitochondrial membrane potential. It was confirmed that the mitochondrial membrane potential was destroyed in the group treated with Tacrine alone, and the pattern was reversed when treated with RG (Figure 3). Thus, it can be seen that RG prevents mitochondrial dysfunction.

Effect of RG on Mitochondrial Dysfunction via AMPK Pathway in Hepatocytes

It is known from previous studies that various cytoprotective substances inhibit mitochondrial dysfunction and oxidative damage through the AMPK-ACC pathway, and since AMPK activation phosphorylates ACC,[35,36] an enzyme necessary for the process of consuming ATP, Phosphorylation can confirm AMPK activation.[37] In this study, AMPK activation was also measured through immunoblotting to investigate the basic mechanism of RG. As a result of treating HepG2 cells with 1000 μg/mL of RG over time, it was observed that RG further reduced phosphorylation of ACC in a time-dependent manner, with the highest expression at 10 minutes. In addition, the highest expression point in AMPK and RG cells was the same at 10 minutes (Figure 4A). In Huh7 cells, the expression points of AMPK and ACC were the highest at 10 minutes, and phosphorylation tended to decrease in a time-dependent manner (Figure 4B).

Effect of RG on AMPK Pathway in Tacrine Hepatotoxicity

LKB1, a cancer suppressor gene, plays a role in regulating cell growth and metabolism, regulating cell responses to energy stress, and linking the state of metabolism with cell growth and regulation of cell polarity.[38] LKB1 protein plays a role in phosphorylating AMP-activated protein kinase (AMPK), a protein that recognizes the energy state in cells, and many metabolic processes in cells are regulated by the interaction between LKB1 and AMPK.[39] As a result of immunoblot analysis to confirm the mechanism by which RG prevents apoptosis caused by tacrine-induced oxidative stress, expression of p-LKB1 was observed and it was confirmed that the expression level of LKB1 increased significantly at 10 minutes (Figure 5A). In addition, in order to confirm that the apoptosis inhibitory action of RG by Tacrine was caused by LKB1, MTT assay was performed by comparing Hela cells lacking HepG2 with LKB1. As a result, cell viability was significantly reduced by tacrine in HepG2 cells, but the survival rate was higher when treated with RG than in the tacrine alone treated group. On the other hand, in Hela cells, the tacrine alone treatment group and the tacrine + RG treatment group had lower survival rates than HepG2 cells. Next, as a result of immunoblot analysis, it was expressed in HepG2 cells, but not in Hela cells (Figure 5B). Therefore, it was found that the apoptosis inhibitory action of RG by tacrine was related to LKB1.
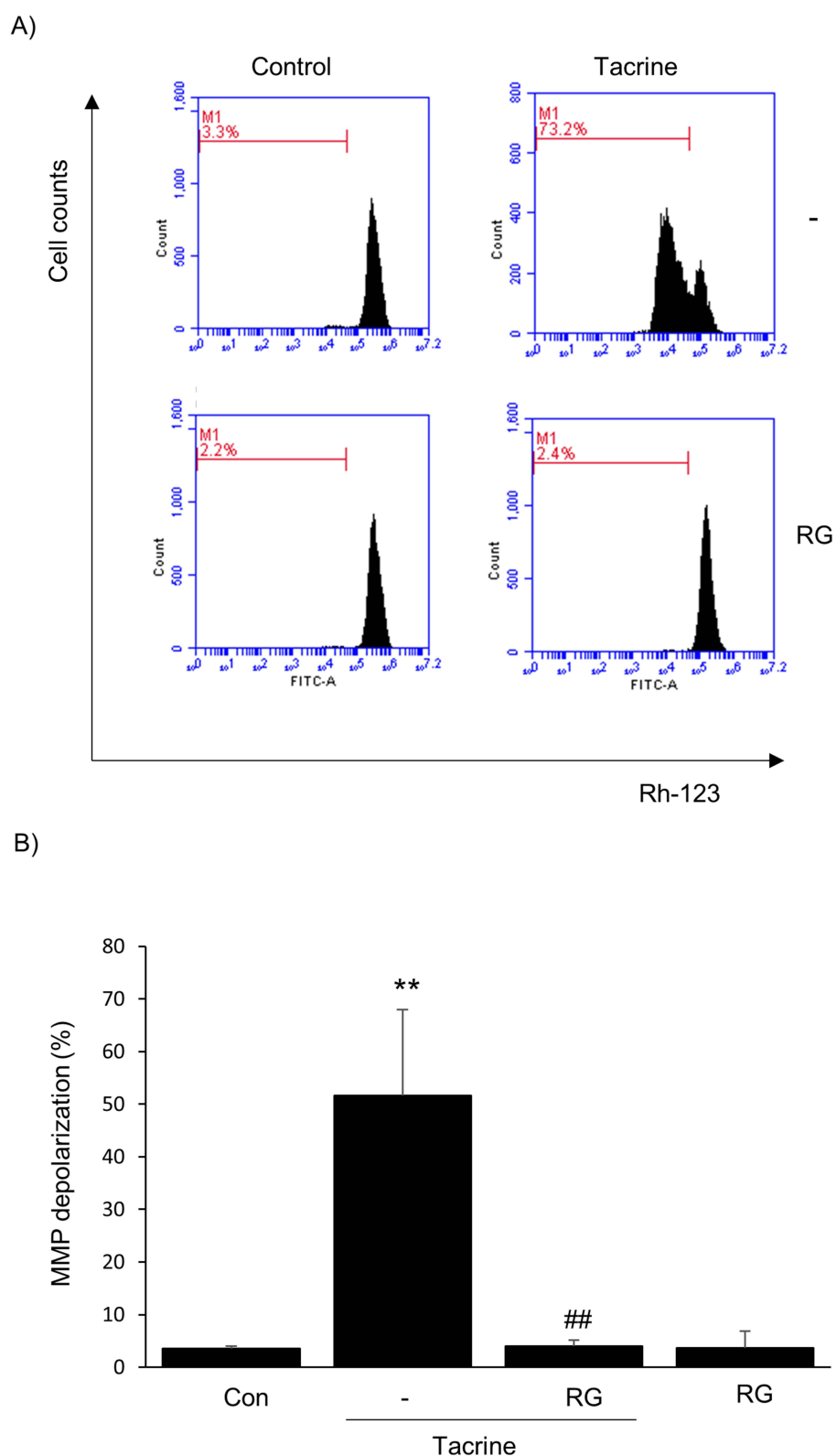
A)

B)

Figure 3 Effect of RG on Mitochondrial Damage in Tacrine Hepatotoxicity. (**A**) Fluorescence-activated cell sorting analysis. (**B**) Mitochondrial membrane potential measurement. HepG2 cells were treated with RG (1000μg/mL) and Tacrine (300μg/mL) for 6 hours. Subsequently, fluorescence intensity was measured by FACS for mitochondrial membrane permeability (MMP) after Rhodamine 123 staining. Data are presented as the average of repeated samples, with error bars representing standard deviations (vs control **p < 0.01; vs Tacrine; ##p < 0.01).
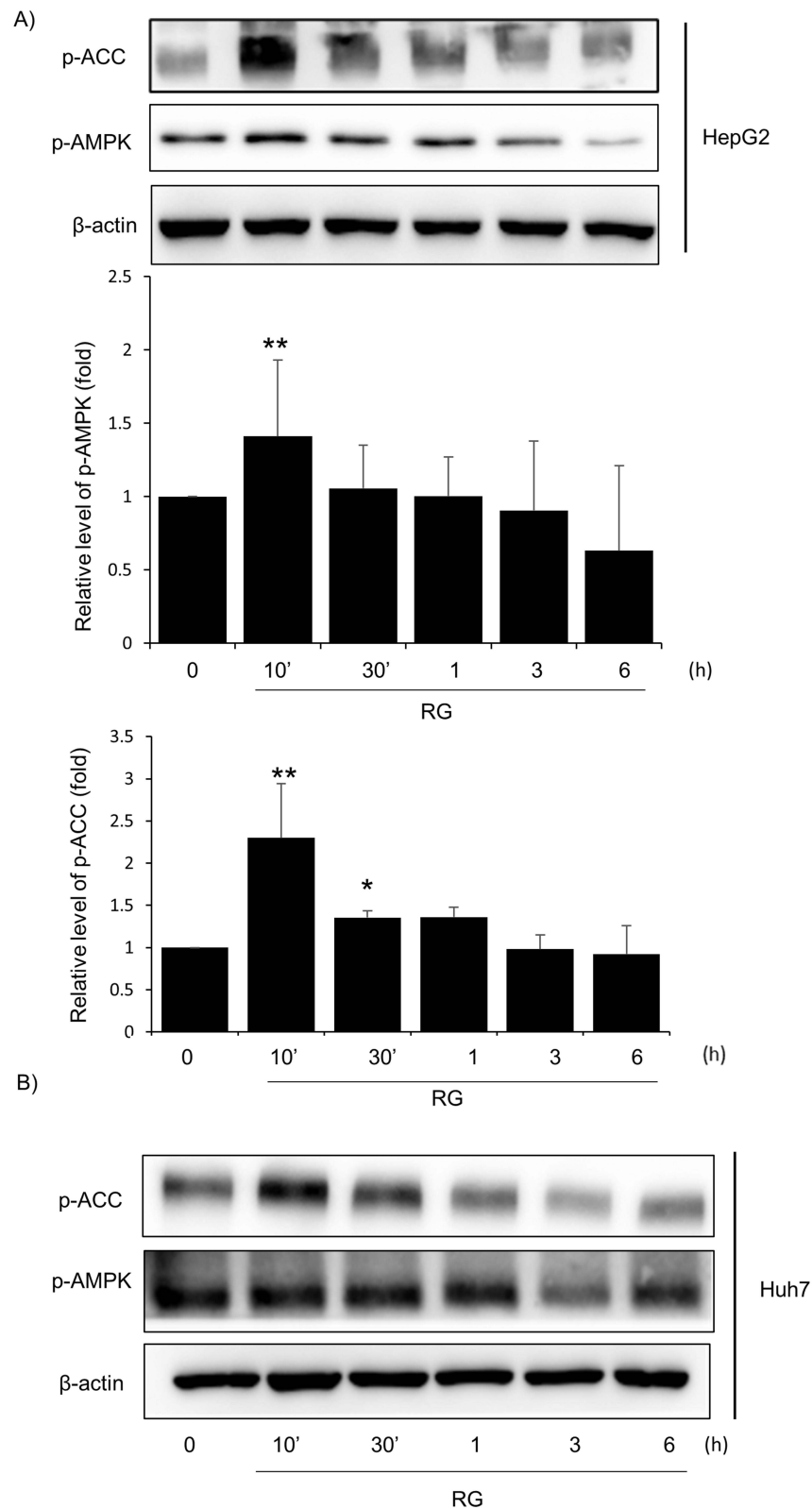
A)

B)

Figure 4 Effect of RG on the AMPK pathway. (**A**) Immunoblot analysis of p-AMPK, p-ACC and β-actin was performed on lysates of HepG2 cells treated for RG times (0, 10', 30', 1 h, 3 h, 6 h). The results were confirmed by repeat experiments below. (**B**) Huh7 cells were treated with RG (0, 10', 30', 1 h, 3 h, 6 h) and immunoblot analysis of p-AMPK, p-ACC and β-actin was performed. Data are presented as the average of repeated samples, with error bars representing standard deviations (vs control *p < 0.05, **p < 0.01).
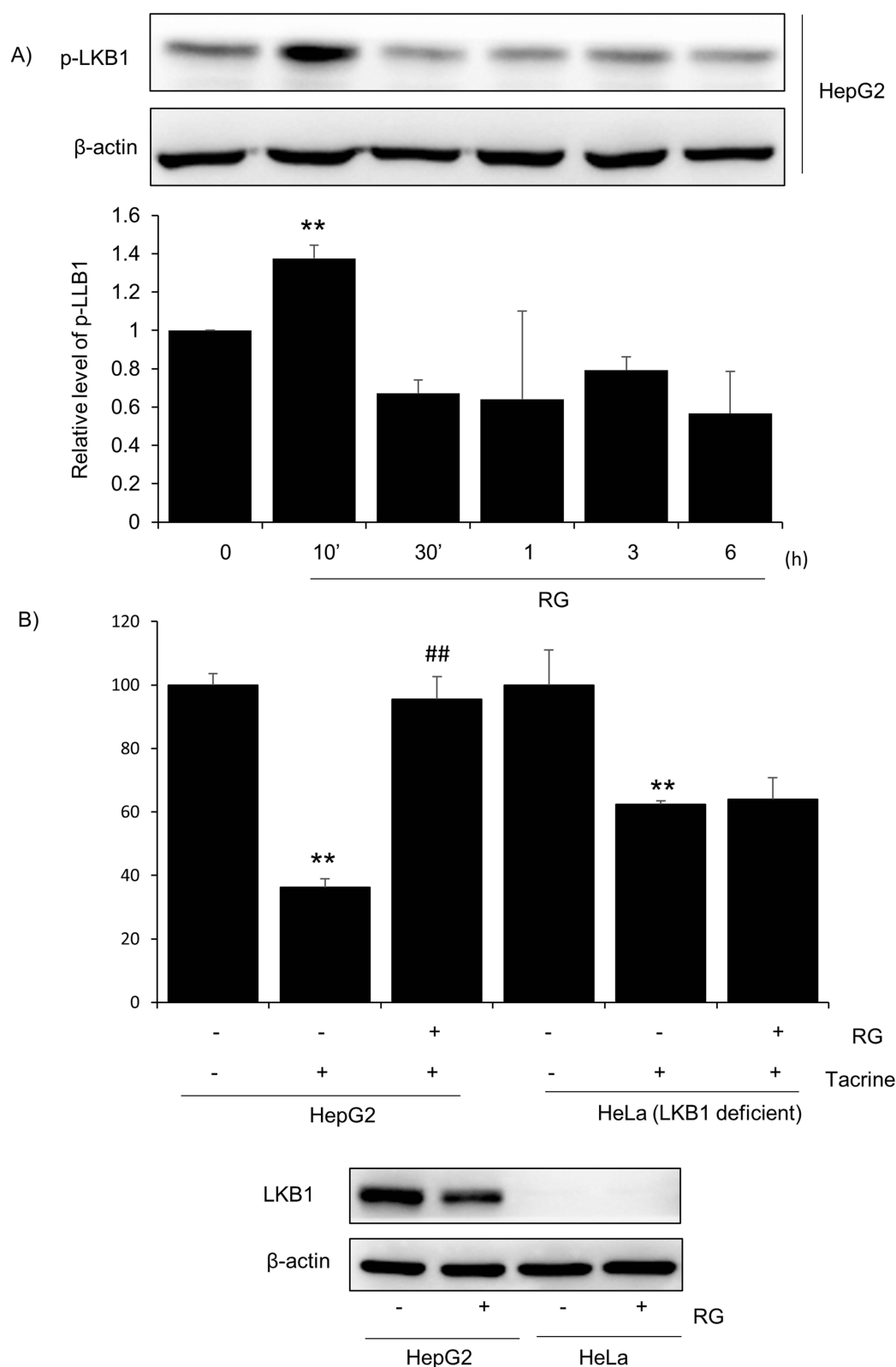
Figure 5 Effect of RG on LKB1 activation. (**A**) Western blotting of key signaling molecules in-volved in the p-LKB1 pathway in HepG2 cells. HepG2 cells were treated with RG (1000μg/mL) for the indicated times. β-actin used as loading control. Results are representative of three independent experiments. Relative protein Levels represent mean ± SD. (**p < 0.01). (**B**) Effect of RG on Tacrine apoptosis on HepG2 and LKB1-deficient HeLa cells. Cells were co-treated with Tacrine 300 μg/mL and 1000 μg/mL RG for 6 hours and MTT test was performed to measure cell viability. Graphs represent mean ± SD. From three independent experiments presented as percentage of control (**p < 0.01 vs vehicle-treated control group; ##P<0.01 vs tacrine-treated group). Western blotting of LKB1 on HepG2 cells and LKB1-deficient HeLa cells RG treatment for 3 h (below).

Effect of RG on p-YAP Pathway Activation

The Hippo signaling pathway plays a crucial role in various biological processes, including organ growth, stem cell function, angiogenesis, and tumor growth suppression.[40] This pathway, especially the Hippo-YAP axis, is significantly implicated in oxidative stress responses. Notably, numerous studies highlight the role of Yes-associated protein (YAP), a transcriptional activator, in mediating signals induced by oxidative stress.[41] Furthermore, both intracellular and extracellular factors activate the Hippo pathway through non-cellular mechanisms.[41] This activation is regulated by upstream kinases like LATS1/LATS2, which modulate localization and protein stability via phosphorylation.[42] Therefore, in this study, Large Tumor Suppressor Kinase 1 (LATS1) and YAP, proteins related to the Hippo-YAP pathway, were observed by treating HepG2 cells with 1000 μg/mL RG over time as an experimental method for immunoblotting analysis. As a result, the phosphorylation of LATS1, a top factor of YAP, increased at 10 minutes and was the most significant, and RG decreased p-YAP in a time-dependent manner. Phosphorylation of YAP increased at 1 h (Figure 6A). In tumor-suppressor-free HeLa cells and HepG2 cells treated with RG, p-LATs1 and p-YAP were expressed in HepG2 cells but weakly in LKB1-deficient Hela cells. On the other hand, phosphorylation of YAP was also well expressed in HeLa cells (Figure 6B).

Effect of RG on p-YAP Pathway Activation

Next, we confirmed the effect of RG on the liver injury induced by tacrine in rats. Oral injections of tacrine for 1 day significantly induced liver damage, as assessed by blood biochemistry and histology (Figure 7A and B). However, the oral pretreatment of RG and silymarin (a positive control) markedly inhibited the induction of liver damage by tacrine.

Discussion

In this study, we successfully demonstrated the protective effects of red ginseng against tacrine-induced hepatotoxicity by integrating network analysis and experimental validations. Although tacrine is a still effective intervention for the treatment of Alzheimer's disease; however, its clinical use has been hampered by hepatotoxicity. Finding a therapeutic agent that can protect against this side effect is of great importance. Our comprehensive approach enabled us to clarify the hepatoprotective effects and the core mechanisms behind RG. Specifically, the network pharmacological analysis revealed the potential of RG in mitigating oxidative liver injury, identifying its key targets and potential active compounds. These findings were systematically validated through comprehensive experiments. In cells, RG successfully inhibited the oxidative stress induced by tacrine as mediated with the AMPK activation and Hippo-YAP pathways. In rats, RG also inhibited the ability of tacrine to induce the hepatotoxicity. Our research highlights the potential for improving the safety profile of tacrine in the context of Alzheimer's treatment.

Our network pharmacology analysis identified 42 red ginseng ingredients and 83 key protein targets that interacted with two or more red ginseng ingredients. Approximately 25% of these key targets overlapped with oxidative liver injury, highlighting red ginseng's potential as a protective component against oxidative liver injury. Further analysis revealed 17 ginseng ingredients that were significantly associated with oxidative liver injury, with Notoginsenoside R1, Ginsenoside Rh2, and Ginsenoside Rb1 showing the highest overlap ratio. The compound-target network constructed by integrating the identified ingredients, protein targets, and associated pathways revealed a complex interplay between red ginseng ingredients and their targets, involving several signaling pathways such as the TNF, MAPK, PI3K-Akt, Toll-like receptor, NF-Kappa B, JAK-STAT, and AMPK pathways. These results demonstrate the value of network pharmacology in identifying key targets and relevant pathways involved in the protective effects of red ginseng against tacrine-induced hepatotoxicity.

The next, this study is first examined the hepatotoxicity of tacrine in HepG2 cells. To investigate the cytoprotective effect of Tacrine As a result of immunoblot assay after treatment of HepG2 cells with tacrine, the expression of procase-3 protein was decreased, but RG significantly suppressed it. Further observation with a fluorescence microscope showed that the Tacrine-treated group tended to increase compared to the other groups in the Pi staining, which showed intense fluorescence as the cell membrane was destroyed, and the cytoprotective effect was shown when RG was administered.
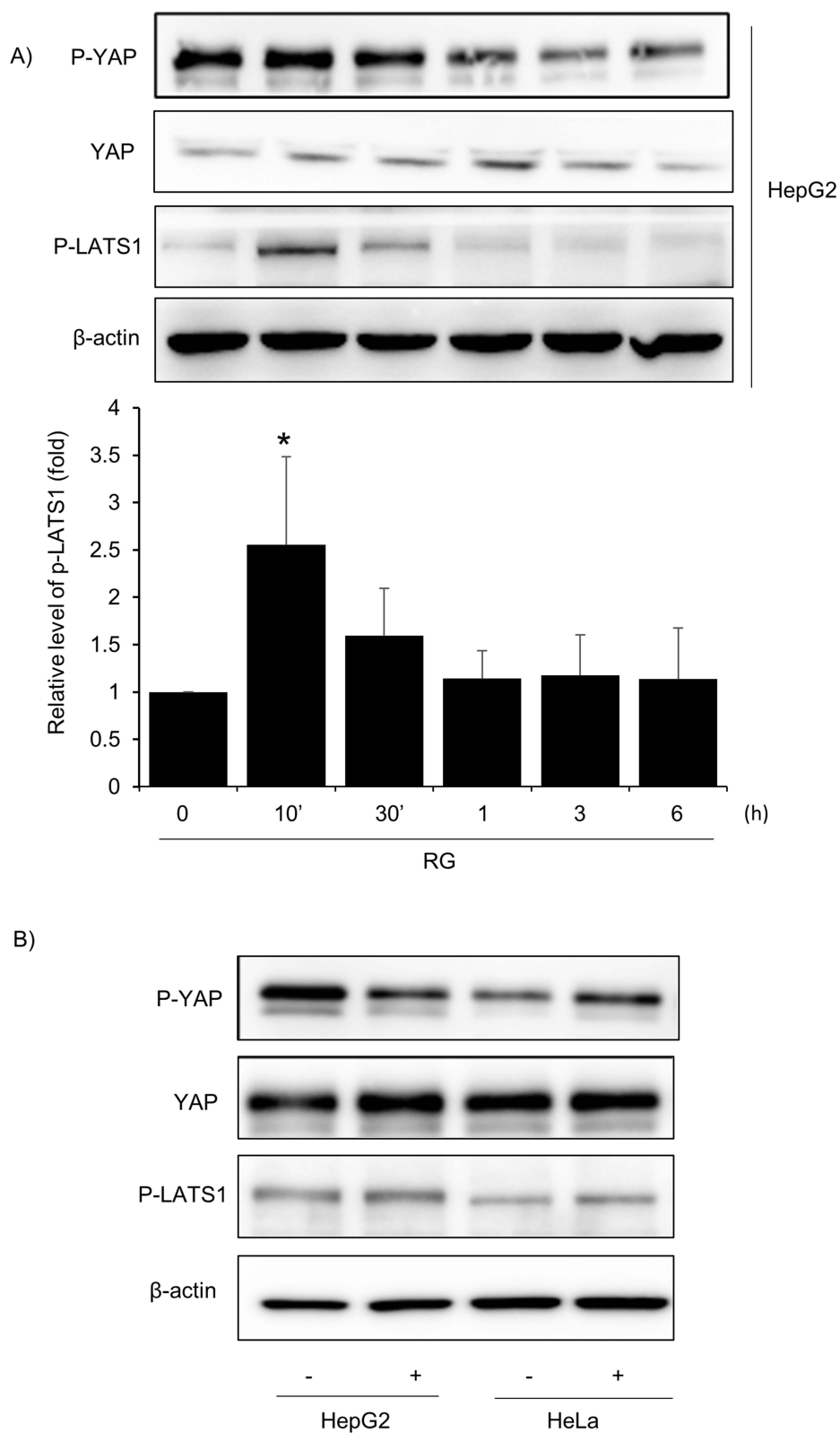
A) P-YAP

YAP

P-LATS1

β-actin

HepG2

Figure 6 Effect of red RG on YAP signal. (**A**) Phosphorylation of YAP and LATS1. Immunoblot analysis was performed on HepG2 cells treated with RG (1000 μg/mL) over time. (**B**) Effects of RG on YAP and LATS1 in LKB1-deficient HeLa cells determined by Western blotting. Data are pre-sented as mean of replicate samples with error bars representing standard deviation (vs control *p < 0.05).
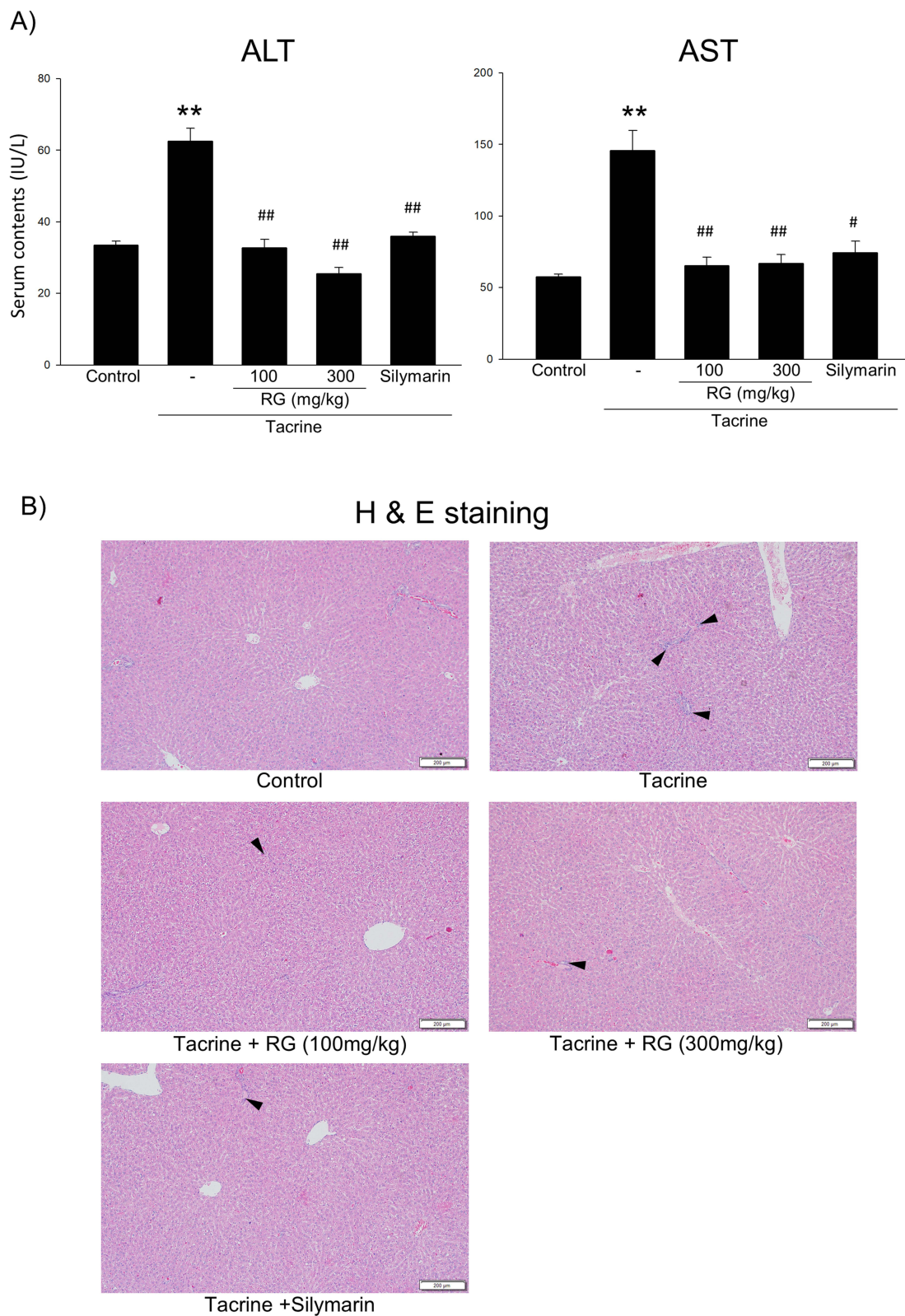
A)

B)

H & E staining

Figure 7 Effects of RG on Tacrine-induced liver injury in rats. 100 and 300 mg/kg RG or 200 mg Silymarin were orally administrated to rats for three consecutive days. Subsequently, 30mg/kg tacrine was injected orally. (**A**) Serum ALT and AST level in rats confirmed the effect of RG on liver injury. The data represent the mean ± S.E.M. (**p < 0.01 between the vehicle control; ###p < 0.01, #p < 0.05 between tacrine treatments). (**B**) Histo-chemical analysis of liver tissue in rats was performed by H&E staining (bar = 200μm). Arrows indicate the degeneration of hepatocytes.

In addition, as a result of measuring MMP, it was found that RG inhibits mitochondrial damage and dysfunction during tacrine treatment and has a cytoprotective effect.

AMPK is an important kinase in the regulation of energy homeostasis and is involved in multiple signaling pathways. AMPK activation is known to promote mitochondrial function, fatty acid and cholesterol synthesis, suppress inflammation, and play an important regulatory role in the progression of cellular aging.[43] In this study, in order to confirm that RG has a cytoprotective effect by activating AMPK from hepatotoxicity by Tacrine and protecting the mitochondrial membrane, immunoblot assay was performed after treating RG at different times. Induced mitochondrial dysfunction was observed with a tendency to decrease phosphorylation in a time-dependent manner. Furthermore, it was observed that the phosphorylation of LKB1 and ACC, which are upstream and downstream factors of AMPK, also decreased.

Previously, tacrine is known to cause liver toxicity even though it is a treatment for dementia, and in fact, it was found that there is liver toxicity in this study. However, it was found that hepatoprotective effect appeared when RG was simultaneously treated, and hepatoprotective effect was similar to that of the control group, indicating that RG was effective in hepatotoxicity. In addition, milk thistle (Silybum marianum) is a plant used for disease treatment and liver disorders-related research, and in the past few years, silymarin has been considered as a hepatoprotective agent to treat various liver diseases (hepatitis, cirrhosis) in humans. and as an antioxidant due to its anti-inflammatory effect.[44] Accordingly, it was found that the hepatotoxic effect was similarly alleviated when compared to RG when co-treated with tacrine. Therefore, it is considered that red ginseng can serve as a therapeutic agent that can improve the safety and efficacy of Alzheimer's disease treatment by alleviating the hepatotoxic effect of tacrine.

Conclusion

This study highlights the potential of red ginseng as a promising agent in mitigating tacrine-induced hepatotoxicity, an obstacle in the treatment of Alzheimer's disease. Through a novel integration of network pharmacology and empirical validation, we have demonstrated red ginseng's ability to protect against oxidative liver injury, enhancing mitochondrial function and reducing oxidative stress. These findings, supported by both in vitro and in vivo experiments, suggest a pivotal role for red ginseng in improving the safety profile of tacrine-based therapies. Moving forward, our research can contribute incorporating natural compounds like red ginseng into Alzheimer's disease treatment strategies, potentially leading to more effective and safer therapeutic options.

Abbreviations

ANOVA, one-way analysis of variance; CTI, compound-target interactions; DMEM, Dulbecco's modified Eagle's medium; DMSO, Dimethyl sulfoxide; FACS, Fluorescence-activated cell sorting; FBS, fetal bovine serum; KEGG, Kyoto Encyclopedia of Genes and Genomes; LATS1, phospho-large tumor suppressor; LKB1, phospho-liver kinase B1; OMIM, Online Mendelian Inheritance in Man; PI, propidium iodide; RG, Red ginseng; SDS-PAGE, sodium dodecyl sulfate-polyacrylamide gel electrophoresis.

Ethics Approval and Consent to Participate

The animal experimentation procedures of this study were approved and monitored by the Institutional Animal Care and Use Committee of Daegu Haany University (Number: DHU-2022-062).

Disclosure

The authors report no conflicts of interest in this work.

References

1. Patterson C. World Alzheimer report 2018. 2018.;
2. Liu S, Li C, Shi Z, et al. Caregiver burden and prevalence of depression, anxiety and sleep disturbances in A lzheimer's disease caregivers in C hina. *J Clin Nurs*. 2017;26(9–10):1291–1300. doi:10.1111/jocn.13601
3. Greenblatt H, Kryger G, Lewis T, Silman I, Sussman J. Structure of acetylcholinesterase complexed with (−)-galanthamine at 2.3 Å resolution. *FEBS Lett*. 1999;463(3):321–326. doi:10.1016/S0014-5793(99)01637-3
4. Bartus RT, Dean RL III, Beer B, Lippa AS. The cholinergic hypothesis of geriatric memory dysfunction. *Science*. 1982;217(4558):408–414. doi:10.1126/science.7046051
5. Watkins PB, Zimmerman HJ, Knapp MJ, Gracon SI, Lewis KW. Hepatotoxic effects of tacrine administration in patients with Alzheimer's disease. *JAMA*. 1994;271(13):992–998. doi:10.1001/jama.1994.03510370044030
6. Mitra S, Muni M, Shawon NJ, et al. Tacrine derivatives in neurological disorders: focus on molecular mechanisms and neurotherapeutic potential. *Oxid Med Cell Longev*. 2022;2022:1–22. doi:10.1155/2022/7252882
7. Kim J-H. Pharmacological and medical applications of Panax ginseng and ginsenosides: a review for use in cardiovascular diseases. *J Ginseng Res*. 2018;42(3):264–269. doi:10.1016/j.jgr.2017.10.004
8. J-N H, Liu Z, Wang Z, et al. Ameliorative effects and possible molecular mechanism of action of black ginseng (Panax ginseng) on Acetaminophen-mediated liver injury. *Molecules*. 2017;22(4):664. doi:10.3390/molecules22040664
9. Cho I-H. Effects of Panax ginseng in neurodegenerative diseases. *J Ginseng Res*. 2012;36(4):342. doi:10.5142/jgr.2012.36.4.342
10. Kim JH, Hahm DH, Yang DC, Kim JH, Lee HJ, Shim I. Effect of crude saponin of Korean red ginseng on high-fat diet-induced obesity in the rat. *J Pharmacol Sci*. 2005;97(1):124–131. doi:10.1254/jphs.FP0040184
11. Park SM, Jung EH, Kim JK, et al. 20S-Protopanaxadiol, an aglycosylated ginsenoside metabolite, induces hepatic stellate cell apoptosis through liver kinase B1–AMP-activated protein kinase activation. *J Ginseng Res*. 2017;41(3):392–402. doi:10.1016/j.jgr.2017.01.012
12. Kim YW, Bak S-B, Song YR, Kim C-E, Lee W-Y. Systematic exploration of therapeutic effects and key mechanisms of Panax ginseng using network-based approaches. *J Ginseng Res*. 2024. doi:10.1016/j.jgr.2024.01.005
13. Kim K, Nam KH, Yi SA, Park JW, Han J-W, Lee J. Ginsenoside Rg3 induces browning of 3T3-L1 adipocytes by activating AMPK signaling. *Nutri*. 2020;12(2):427. doi:10.3390/nu12020427
14. Han JY, Lee S, Yang JH, et al. Korean red Ginseng attenuates ethanol-induced steatosis and oxidative stress via AMPK/Sirt1 activation. *J Ginseng Res*. 2015;39(2):105–115. doi:10.1016/j.jgr.2014.09.001
15. Hossain KN, Islam MS, Rahman SH, et al. In vitro antioxidant and in vivo hepatoprotective properties of Wissadula periplocifolia extract. *ACS omega*. 2023;8(49):47001–47011. doi:10.1021/acsomega.3c06614
16. El-Ghffar EA A, El-Nashar HA, Eldahshan OA, Singab ANB. GC-MS analysis and hepatoprotective activity of the n-hexane extract of Acrocarpus fraxinifolius leaves against paracetamol-induced hepatotoxicity in male albino rats. *Pharm Biol*. 2017;55(1):441–449. doi:10.1080/13880209.2016.1246575
17. Hopkins AL. Network pharmacology: the next paradigm in drug discovery. *Nat Chem Biol*. 2008;4(11):682–690. doi:10.1038/nchembio.118
18. Zhang G-B, Q-y L, Q-l C, S-b S. Network pharmacology: a new approach for Chinese herbal medicine research. *Evid Based Compl Alter Med*. 2013;2013:1.
19. Zhang R, Zhu X, Bai H, Ning K. Network pharmacology databases for traditional Chinese medicine: review and assessment. *Front Pharmacol*. 2019;10:123. doi:10.3389/fphar.2019.00123
20. Bak SB, Song YR, Bae SJ, Lee WY, Kim YW. Integrative approach to uncover antioxidant properties of Bupleuri Radix and its active compounds: multiscale interactome-level analysis with experimental validation. *Free Radic Biol Med*. 2023;199:141–153. doi:10.1016/j.freeradbiomed.2023.02.016
21. Lee WY, Lee CY, Lee JS, Kim CE. Identifying Candidate flavonoids for non-alcoholic fatty liver disease by network-based strategy. *Front Pharmacol*. 2022;13:892559. doi:10.3389/fphar.2022.892559
22. Wishart DS, Feunang YD, Guo AC, et al. DrugBank 5.0: a major update to the DrugBank database for 2018. *Nucleic Acids Res*. 2018;46(D1):D1074–D1082. doi:10.1093/nar/gkx1037
23. Wang Y, Zhang S, Li F, et al. Therapeutic target database 2020: enriched resource for facilitating research and early development of targeted therapeutics. *Nucleic Acids Res*. 2020;48(D1):D1031–D1041. doi:10.1093/nar/gkz981
24. Szklarczyk D, Santos A, Von Mering C, Jensen LJ, Bork P, Kuhn M. STITCH 5: augmenting protein–chemical interaction networks with tissue and affinity data. *Nucleic Acids Res*. 2016;44(D1):D380–D384. doi:10.1093/nar/gkv1277
25. Huang Y, Fang J, Lu W, et al. A systems pharmacology approach uncovers wogonoside as an angiogenesis inhibitor of triple-negative breast cancer by targeting hedgehog signaling. *Cell Chem Biol*. 2019;26(8):1143–1158. e6. doi:10.1016/j.chembiol.2019.05.004
26. Shannon P, Markiel A, Ozier O, et al. Cytoscape: a software environment for integrated models of biomolecular interaction networks. *Genome Res*. 2003;13(11):2498–2504. doi:10.1101/gr.1239303
27. Malhi H, Gores GJ. Cellular and molecular mechanisms of liver injury. *Gastroenterology*. 2008;134(6):1641–1654. doi:10.1053/j.gastro.2008.03.002
28. Zeng L, Tang WJ, Yin JJ, Zhou BJ. Signal transductions and nonalcoholic fatty liver: a mini-review. *Int J Clin Exp Med*. 2014;7(7):1624.
29. Russell JO, Camargo FD. Hippo signalling in the liver: role in development, regeneration and disease. *Nat Rev Gastroenterol Hepatol*. 2022;19(5):297–312. doi:10.1038/s41575-021-00571-w
30. Kuleshov MV, Jones MR, Rouillard AD, et al. Enrichr: a comprehensive gene set enrichment analysis web server 2016 update. *Nucleic Acids Res*. 2016;44(W1):W90–W97. doi:10.1093/nar/gkw377
31. Dong G-Z, Jang EJ, Kang SH, et al. Red ginseng abrogates oxidative stress via mitochondria protection mediated by LKB1-AMPK pathway. *BMC Compl Altern Med*. 2013;13:1–9. doi:10.1186/1472-6882-13-64
32. Ki SH, Yang JH, Ku SK, Kim SC, Kim YW, Cho IJ. Red ginseng extract protects against carbon tetrachloride-induced liver fibrosis. *J Ginseng Res*. 2013;37(1):45. doi:10.5142/jgr.2013.37.45
33. Park SM, Ki SH, Han NR, et al. Tacrine, an oral acetylcholinesterase inhibitor, induced hepatic oxidative damage, which was blocked by liquiritigenin through GSK3-beta inhibition. *Biol Pharm Bull*. 2015;38(2):184–192. doi:10.1248/bpb.b14-00430
34. Boudreau MW, Peh J, Hergenrother PJ. Procaspase-3 overexpression in cancer: a paradoxical observation with therapeutic potential. *ACS Chem Biol*. 2019;14(11):2335–2348. doi:10.1021/acschembio.9b00338

35. Li K, Chen L, Lin Z, et al. Role of the AMPK/ACC signaling pathway in TRPP2-mediated head and neck cancer cell proliferation. *Biomed Res Int*. 2020;2020:1.

36. Katashima CK, de Oliveira Micheletti T, Braga RR, et al. Evidence for a neuromuscular circuit involving hypothalamic interleukin-6 in the control of skeletal muscle metabolism. *Sci Adv*. 2022;8(30):eabm7355. doi:10.1126/sciadv.abm7355

37. Kim D, Park SM, Byun SH, Park CA, Cho IJ, Kim SC. Hepato-protective effects of Daucus carota L. root ethanol extract through activation of AMPK in HepG2 cells. *Herb Formula Sci*. 2018;26(4):329–340.

38. T-t L, H-b Z. LKB1 and cancer: the dual role of metabolic regulation. *Biomed Pharmacother*. 2020;132:110872. doi:10.1016/j.biopha.2020.110872

39. Ciccarese F, Zulato E, Indraccolo S. LKB1/AMPK pathway and drug response in cancer: a therapeutic perspective. *Oxid Med Cell Longev*. 2019;2019:1–16. doi:10.1155/2019/8730816

40. Park J. The mechanism and efficacy of targeting YAP-TEAD in colorectal cancer. Graduate School, Yonsei University; 2018. Available from: https://ir.ymlib.yonsei.ac.kr/handle/22282913/159957. Accessed February 21, 2024.

41. Shao D, Zhai P, Del Re DP, et al. A functional interaction between Hippo-YAP signalling and FoxO1 mediates the oxidative stress response. *Nat Commun*. 2014;5(1):3315. doi:10.1038/ncomms4315

42. Boopathy G, Hong W. Role of hippo pathway-YAP/TAZ signaling in angiogenesis. *Front Cell Dev Biol*.2019;7:49. doi:10.3389/fcell.2019.00049

43. Hsu -C-C, Peng D, Cai Z, Lin H-K. AMPK signaling and its targeting in cancer progression and treatment. *Elsevier*. 2022;2022:52–68.

44. Owatari MS, Jesus GFA, Brum A, et al. Sylimarin as hepatic protector and immunomodulator in Nile tilapia during Streptococcus agalactiae infection. *Fish Shellfish Immunol*. 2018;82:565–572. doi:10.1016/j.fsi.2018.08.061